Int. J. Heat Mass Transfer. Vol. 31, No. 6, pp. 1299–1308, 1988
Printed in Great Britain

0017–9310/88 $3.00 + 0.00
Pergamon Press plc

Numerical analysis of the Graetz problem with natural convection in a uniformly heated horizontal tube

F. C. CHOU
Department of Mechanical Engineering, National Central University, Chungli, Taiwan, R.O.C.

and

G. J. HWANG†
Department of Power Mechanical Engineering, National Tsing Hua University, Hsinchu, Taiwan, R.O.C.

(*Received* 11 *June* 1987 *and in final form* 1 *December* 1987)

Abstract—Without the aid of the large Prandtl number assumption, the Graetz problem with the effect of natural convection in a uniformly heated horizontal tube is studied numerically by a relatively novel vorticity–velocity method. Variations in local friction factor and Nusselt number with Rayleigh number are shown for Prandtl numbers, $Pr = 5$, 2 and 0.7. Comparing with the available experimental data for water, the present results for $Pr = 5$ show a better agreement than those with $Pr \to \infty$. The asymptotic solutions for $z \to \infty$ are further compared against the existing analytical and experimental data. A reasonably good agreement is observed.

INTRODUCTION

BECAUSE of practical interest, the combined free and forced laminar convection in tubes had been studied by many investigators. Experimental data are rather abundant in both horizontal and inclined tubes. In view of the various working fluids used in the literature, glycerol [1], the mixture of water and glycerol [1, 2], and ethylene glycol [3–5] are classified as large Prandtl number fluids; and, air [6–10], and nitrogen [6] small Prandtl number fluids, while the Prandtl numbers of water [1–4, 10–19] and ethyl alcohol [1, 2] are moderate. Some of these studies include data for entrance flow [1, 2, 5, 6, 9, 11–19].

Numerous analytical solutions for this problem were proposed first in the fully developed flow. Generally, the uniform wall heat flux boundary condition with either a zero ('ZC') [20] or infinite ('IC') [21, 22] value of the peripheral thermal conductivity was utilized. However, the fully developed flow can only be established in a long tube. Although the flow and heat transfer characteristics of entrance flow with significant natural convection effects are practically important, the numerical data are available only in limited cases due to the complexities arising from the three-dimensionality of the flow. A large Prandtl number assumption was frequently used [4, 23–27] to avoid the difficulty, but the results are obviously unsuitable for both moderate and small Prandtl number fluids, such as water and gases. The perturbation method [28] was known to be practical only in the regime where the natural convection effect is sufficiently small. The numerical solutions solving three-dimensional elliptic governing equations [29] needed prohibitively large computer time and thus were unsuitable for engineering applications. By a slight modification to the primitive variable calculation described by Patankar and Spalding [30], the buoyancy effects in the entrance region of horizontal rectangular channels were studied by Abou-Ellail and Morcos [31]. The available methods for solving the primitive variable formulation need extra programming and storage effort (e.g. the use of staggered grids) and underrelaxation of the pressure-correction equation as discussed in Farouk and Fusegi [32].

The formulation of the Navier–Stokes equations employing the vorticity–velocity components has been used for two-dimensional hydrodynamic stability problems [33, 34]. References [35, 36] have also used the vorticity–velocity method for predicting three-dimensional flows along vertical and horizontal square ducts, respectively. In the present study the vorticity–velocity formulation of the Navier–Stokes equations and the corresponding numerical scheme are extended to the problem in a circular tube by using cylindrical coordinates, and the flow and heat transfer characteristics of the thermal entrance flow in a horizontal tube can be further investigated for moderate and small Prandtl number fluids.

† Author to whom correspondence should be addressed.

NOMENCLATURE

a, d	tube radius and diameter
C	constant, $(a^2/\mu\bar{W}_f)\partial P_f/\partial Z$
Gr	Grashof number, $g\beta\theta_c a^3/\nu^2$
Gr^+	Grashof number used by Patankar *et al.* [37], $g\beta Q' a^3/k\nu^2$
f	friction coefficient, $2\bar{\tau}_w/(\rho\bar{W}'^2)$
g	gravitational acceleration
$\bar{h}$	average heat transfer coefficient
k	thermal conductivity
M, N	number of divisions in the r- and ϕ-directions, respectively
Nu	local Nusselt number, $\bar{h}d/k$
P, P_f	pressure deviation and pressure for fully developed laminar flow before thermal entrance, respectively
p	dimensionless quantity for P
Pe	Peclet number, $Pr\,Re$
Pr	Prandtl number, ν/α
Q'	rate of heat transfer per unit axial length used by Patankar *et al.* [37]
q_w	uniform heat flux at wall
R, ϕ, Z	cylindrical coordinates
r, ϕ, z	dimensionless cylindrical coordinates
Ra	Rayleigh number, $Pr\,Gr$
Ra^*, Ra^*_{fm}	Rayleigh number based on bulk temperature difference and that evaluated at film temperature used by Morcos and Bergles [3], $g\beta(\bar{T}_w - T_b)d^3/\nu\alpha$
Re	Reynolds number, $\bar{W}'d/\nu$
$Re\,Ra_\tau$	parameter used in refs. [8, 22], $(\bar{W}'d/\nu)[\beta g(\partial T/\partial Z)a^4/\nu\alpha]$
T, T_0	local temperature and uniform fluid temperature at entrance, respectively
U, V, W	velocity components in the R-, ϕ-, Z-directions due to buoyancy effect
u, v, w	dimensionless quantities for U, V and W
W_f	fully developed axial velocity before thermal entrance
w_f	dimensionless quantity for W_f
W', w'	axial velocity in the thermal entrance region, $W_f + W$ and its dimensionless quantity, $w_f + 4Ra\,w$.

Greek symbols

α	thermal diffusivity
β	coefficient of thermal expansion
ε	prescribed error defined in equation (18)
θ	dimensionless temperature difference, $(T - T_0)/\theta_c$
θ_c	characteristic temperature, $q_w a/k$
$\theta_b, \bar{\theta}_w$	dimensionless bulk and average wall temperature, respectively
μ	viscosity
ν	kinematic viscosity
ξ	axial-direction vorticity defined in equation (8)
ρ	density
τ	shear stress.

Subscripts

c	characteristic quantity
fm	value evaluated at fluid film temperature $(\bar{T}_w + T_b)/2$
w	value at wall
0	condition for pure forced convection.

Superscript

	average value.

Other symbol

$\nabla^2_{r,\phi}$	Laplacian operator, $\partial^2/\partial r^2 + (1/r)\partial/\partial r + (1/r^2)\partial^2/\partial\phi^2$.

THEORETICAL ANALYSIS

Consider a steady, hydrodynamically fully developed laminar flow in a horizontal circular tube, the tube wall being heated with a uniform heat flux at $Z \geqslant 0$. The physical configuration is shown in Fig. 1. The well-known classical Graetz problem is extended by including the natural convection effect by using the Boussinesq approximation. Neglecting the viscous dissipation and compression work and introducing the following dimensionless variables and parameters:

$$r = R/a, \qquad z = Z/(2a\,Pe)$$
$$u = U/U_c, \qquad v = V/U_c$$
$$w_f = W_f/\bar{W}_f, \qquad w = W/(4Ra\,\bar{W}_f)$$
$$p = P/(\rho U_c \nu/a), \quad \theta = (T - T_0)/\theta_c$$
$$Gr = g\beta\theta_c a^3/\nu^2, \quad Pr = \nu/\alpha$$
$$Re = \bar{W}_f(2a)/\nu, \quad Pe = Pr\,Re$$
$$U_c = Gr\,\nu/a, \quad \theta_c = q_w a/k \qquad (1)$$

the governing equations for continuity, momentum and energy can be written as

$$\frac{\partial u}{\partial r} + \frac{1}{r}\frac{\partial v}{\partial \phi} + \frac{\partial w}{\partial z} = 0 \qquad (2)$$

$$\frac{Ra}{Pr}\left(u\frac{\partial u}{\partial r} + \frac{v}{r}\frac{\partial u}{\partial \phi} - \frac{v}{r^2} + w\frac{\partial u}{\partial z}\right) + \frac{1}{4Pr}w_f\frac{\partial u}{\partial z}$$
$$= -\frac{\partial p}{\partial r} + \nabla^2_{r,\phi}u - \frac{u}{r} - \frac{2}{r^2}\frac{\partial v}{\partial \phi} + \theta\cos\phi \qquad (3)$$

$$\frac{Ra}{Pr}\left(u\frac{\partial v}{\partial r}+\frac{v}{r}\frac{\partial v}{\partial \phi}+\frac{uv}{r}+w\frac{\partial v}{\partial z}\right)+\frac{1}{4Pr}w_f\frac{\partial v}{\partial z}$$
$$=-\frac{\partial p}{r\partial \phi}+\nabla^2_{r,\phi}v+\frac{2}{r^2}\frac{\partial u}{\partial \phi}-\frac{v}{r}-\theta\sin\phi \quad (4)$$

$$\frac{Ra}{Pr}\left(u\frac{\partial w}{\partial r}+\frac{v}{r}\frac{\partial w}{\partial \phi}+w\frac{\partial w}{\partial z}\right)+\frac{1}{4Pr}\left(u\frac{\partial w_f}{\partial r}+w_f\frac{\partial w}{\partial z}\right)$$
$$=\left(\frac{-1}{4Pe^2}\right)\frac{\partial p}{\partial z}+\nabla^2_{r,\phi}w \quad (5)$$

$$\nabla^2_r w_f = C \quad (6)$$

$$Ra\left(u\frac{\partial \theta}{\partial r}+\frac{v}{r}\frac{\partial \theta}{\partial \phi}+w\frac{\partial \theta}{\partial z}\right)+\frac{w_f}{4}\frac{\partial \theta}{\partial z}=\nabla^2_{r,\phi}\theta \quad (7)$$

where $w_f = 2(1-r^2)$. Without considering the solution near the vicinity of $Z = 0$ [7, 23–26, 31, 35], the axial viscous and diffusion terms are neglected. Following the assumption made in ref. [36], the axial pressure gradient retained in the equation is independent of r and ϕ. In the present numerical computation, the value of $\partial p/\partial z$ is adjusted to fulfill the global continuity condition at each cross-section. It is noted that the terms on the left-hand side of the momentum equations (3)–(5) can be neglected if the large Prandtl number assumption is applied. Furthermore, equation (5) yields a trivial solution, $w = 0$ and $\partial p/\partial z = 0$ everywhere in view of the fact that $\bar{w} = 0$. Hence the continuity equation (2) is reduced to the two-dimensional form and the resultant governing equations (3)–(7) will be the same as those in refs. [4, 24].

Without the aid of the large Prandtl number assumption, the vorticity–velocity formulation of the governing equations in a tube and its numerical scheme are developed as follows. By introducing the vorticity in the axial direction

$$\xi = \frac{\partial u}{r\partial \phi}-\frac{\partial v}{\partial r}-\frac{v}{r} \quad (8)$$

the governing equations (2)–(4) can be reduced as follows:

$$\nabla^2_{r,\phi}u = \frac{v}{r^2}-\frac{2}{r^2}\frac{\partial u}{\partial \phi}-\frac{1}{r}\frac{\partial^2 w}{\partial \phi \partial z}-\frac{\partial \xi}{\partial r} \quad (9)$$

$$\nabla^2_{r,\phi}v = \frac{u}{r^2}+\frac{2}{r^2}\frac{\partial v}{\partial \phi}-\frac{\partial^2 w}{\partial r \partial z}+\frac{\partial \xi}{r\partial \phi} \quad (10)$$

$$Gr\left(u\frac{\partial \xi}{\partial r}+\frac{v}{r}\frac{\partial \xi}{\partial \phi}+w\frac{\partial \xi}{\partial z}+\xi\frac{\partial u}{\partial r}+\xi\frac{\partial v}{r\partial \phi}+\xi\frac{u}{r}\right.$$
$$\left.+\frac{\partial w}{r\partial \phi}\frac{\partial u}{\partial z}-\frac{\partial w}{\partial r}\frac{\partial v}{\partial z}\right)+\frac{1}{4Pr}\left(w_f\frac{\partial \xi}{\partial z}-\frac{\partial w_f}{\partial r}\frac{\partial v}{\partial z}\right)$$
$$=\nabla^2_{r,\phi}\xi+\frac{\partial \theta}{r\partial \phi}\cos\phi+\frac{\partial \theta}{\partial r}\sin\phi. \quad (11)$$

The pressure terms in equations (3) and (4) are eliminated by a cross-differentiation to obtain the vorticity transport equation (11). Equations (9) and (10) can be derived by differentiating the definition of vorticity (8) with respect to r and ϕ, respectively, and using the continuity equation (2). Equations (9) and (10) are used for solving the cross-sectional velocity components u and v. Because of symmetry, the boundary and initial conditions are stated as follows:

$$u = v = w = 0 \quad \text{and} \quad \partial\theta/\partial r = 1 \quad \text{at } r = 1$$
$$v = \partial u/(r\partial\phi) = \partial w/(r\partial\phi) = \xi = \partial\theta/(r\partial\phi) = 0$$
along symmetry plane, $\phi = 0$ and π
$$u = v = w = \xi = \theta = 0 \text{ at entrance, } z = 0. \quad (12)$$

It is noted that equations (2)–(11) and boundary conditions (12) are singular at $r = 0$. To avoid this difficulty in computation, Cartesian coordinates are used to formulate the equations at this point. Accordingly, the horizontal velocity, the vorticity and horizontal gradients of vertical velocity, axial velocity and temperatures are zero at $r = 0$.

Of practical interest are the computations of the local friction coefficient $f\,Re$ and local Nusselt number Nu from the determined developing velocity and temperature fields along the channel axis z. Following the usual definitions, the expressions for $f\,Re$ and Nu can be written based on the overall force balance for an axial length dZ and the temperature gradient at the wall. The results are expressed as

$$(f\,Re)_0 = 2\bar{\tau}_w/(\rho\bar{W}_f^2)(2a\bar{W}_f/\nu) = 16 = -2C \quad (13)$$

$$f\,Re/(f\,Re)_0 = 1+(\partial P/\partial Z)/(\partial P_f/\partial Z)$$
$$= 1+Ra\,f_1(z)/2 \quad (14)$$

$$(Nu)_1 = \bar{h}(2a)/k_f = 2/(\bar{\theta}_w-\theta_b) \quad (15)$$

where subscript 0 denotes the quantity for pure forced convection

$$f_1(z)[=-(\partial p/\partial z)/(4Pe^2)]$$

is the pressure deviation due to secondary flow generated by the axial momentum. If the large Prandtl number assumption is invoked, the mean axial velocity is kept practically unchanged from that of the pure forced convection [4, 23–26]. Thus, w will be identically zero and $w' = w_f$ as shown in refs. [4, 24].

The Nusselt number may be also obtained by considering an overall energy balance for the axial length dZ as

$$(Nu)_2 = \int_0^{\pi}\int_0^1 (\partial\theta/\partial z)wr\,dr\,d\phi/[2\pi(\bar{\theta}_w-\theta_b)]. \quad (16)$$

Although the mean value of $(Nu)_1$ and $(Nu)_2$ was taken as the final local Nusselt number presented in ref. [24], only the value of $(Nu)_1$ is used in the present study due to a better accuracy as shown in the analytical work by Patankar *et al.* [37] and experimental work by Morcos and Bergles [3].

NUMERICAL METHOD OF SOLUTION

For given values of Ra and Pr, the numerical method of solution for unknown u, v, w, ξ and θ in equations (5)–(11) satisfying boundary condition (12) is briefly described below.

(1) The initial values for velocity components u, v, w and the temperature difference θ are assigned zero at $z \leqslant 0$. Consequently, $\xi = 0$ at $z \leqslant 0$ results from equation (8).

(2) The values of $\partial u/\partial z$ and $\partial v/\partial z$ in equation (11) are calculated by using a two-point backward difference formula. With the known values of u, v, w, w_1, θ, $-(\partial p/\partial z)/(4Pe^2)$ and its cross-sectional spatial derivatives computed by a central difference formula, the new values of w, θ and ξ at the interior points of the next axial position are obtained from equations (5), (7) and (11), respectively, by the Du Fort–Frankel method [4, 26].

(3) Check if the mean axial velocity due to the buoyancy effect $\bar{w}$ is equal to zero. Otherwise, adjust the value of the pressure term $f_1(z) = -(\partial p/\partial z)/(4Pe^2)$ in equation (5) to meet the requirement that $\bar{w} = 0$. Thus the values of the local $f\,Re$ in equation (14) at this axial position can be determined.

(4) By applying boundary conditions $\partial\theta/\partial r = 1$ and $\nabla^2_{r,\phi}\theta = 0$ at the wall, the temperature along the tube wall can be computed by iteration after the temperatures in the interior points are found. Then the Nusselt number $(Nu)_1$ is computed from equation (15).

(5) The values of $\partial^2 w/(r\partial\phi\partial z)$, $\partial^2 w/\partial r\partial z$, $\partial u/(r\partial\theta)$, $\partial v/(r\partial\phi)$, $\partial\xi/\partial r$ and $\partial\xi/(r\partial\phi)$ are calculated from the results obtained in step (2) by using the backward difference formula in the axial direction and a central difference formula in the transverse direction. The elliptic equations (9) and (10) are solved for u and v by an iteration process. During the iteration process, the values of vorticity on the boundary are evaluated simultaneously with u and v in the interior region as

$$\xi_{M+1,j} = (u_{M,j+1} - u_{M,j-1})/(2r_{M+1/2}\Delta\phi) + 2v_{M,j}/\Delta r - v_{M,j}/r_{M+1/2} - \xi_{M,j}. \quad (17)$$

It is noted that equation (17) is obtained by discretizing equation (8) into finite-difference form at the point $(M+1/2, j)$. Initially, the boundary vorticity at the previous axial section was used to compute the current interior vorticity, but this process was found to give an unconverged solution. Finally, equation (17) was used in the present numerical scheme.

(6) The following convergence criterion for the velocity components u and v is used to judge whether or not another iteration is performed

$$\varepsilon = \sum_{i}^{M}\sum_{j}^{N} |(u_{i,j}^{n+1} - u_{i,j}^{n})/u_{i,j}^{n+1}|/(M \times N) < 5 \times 10^{-4} \quad (18)$$

where M and N are the number of divisions in the r- and ϕ-directions, respectively.

(7) By repeating steps (2)–(6), the unknowns u, v, w, ξ and θ at the next axial step can be calculated. By numerical experiments, an optimal step size Δz depends mainly on the magnitude of the Rayleigh number and also the Prandtl number. In the present study, the axial step size Δz ranges from 10^{-5} to 10^{-4}.

A cross-sectional mesh size ($M \times N$) of 20×20 has been found to yield an acceptable accuracy in Hong *et al.* [4] and is used in the present study. The required computer time for solution of one set of Pr and Ra is approximately 500 s for the cases of $Pr = 5$ and $Ra \leqslant 10^5$ and 1500 s for the cases of $Pr = 0.7$ and $Ra \leqslant 3 \times 10^4$ on a CDC cyber 170 system.

RESULTS AND DISCUSSION

The numerical result should be independent of the axial step size Δz. Therefore, a numerical experiment was made and the result is shown in Table 1 for the case of $Pr = 5$ and $Ra = 10^5$. It is seen that the deviations of computed Nu with $\Delta z = 2.5 \times 10^{-5}$ and 5×10^{-5}, at each axial position are less than 0.46%. This independency of the numerical result on Δz also reveals that the two-point backward difference formula employed in this numerical method, does not yield any appreciable error.

The typical developing temperature profiles along the vertical symmetry line ($\phi = 0$ and π) are shown in Fig. 2 for the cases of $Pr = 5$ and 2, and $Ra = 10^5$ at various axial positions. The buoyancy induced secondary flow carries the heated fluid upward along the tube wall and downward along the symmetry plane. Therefore, the temperature at the upper wall ($r = 1.0$, $\phi = 0$) is greater than that at the lower wall ($r = 1.0$, $\phi = \pi$). The temperature distributions along $\phi = 0$ and π develop gradually from the almost symmetric case at $z = 1 \times 10^{-3}$ where the secondary flow is rather weak to the case at $z = 1.25 \times 10^{-2}$ in which a large temperature difference between the upper part (along $\phi = 0$) and the lower part (along $\phi = \pi$) is found due to the development of secondary flow. The effect of Prandtl number on developing temperature profiles can be also investigated by comparison of the results for $Pr = 5$ and 2 shown in Fig. 2. It is seen that the temperature distribution for $Pr = 2$ almost coincides with that of $Pr = 5$ at $z \leqslant 2 \times 10^{-3}$, but at $z = 6 \times 10^{-3}$ and 1×10^{-2} the values of the curves of $Pr = 2$ are higher than those of $Pr = 5$ in the upper part ($\phi = 0$) because the intensity of the secondary flow is stronger for the cases of $Pr = 2$ due to its higher Grashof number rather than that of $Pr = 5$.

Figure 3 shows the development of axial velocity due to the buoyancy effect along the symmetry line ($\phi = 0$ and π) for the cases of $Pr = 5$ and 2 with $Ra = 10^5$ at various axial positions. It is seen that the axial velocity profiles are almost symmetric with respect to the centre $r = 0$ at $z = 1 \times 10^{-3}$ and 2×10^{-3}

Table 1. Nusselt number results obtained by a numerical experiment for Δz ($Pr = 5$, $Ra = 10^5$)

Δz	z					
	1×10^{-3}	2×10^{-3}	4×10^{-3}	6×10^{-3}	8×10^{-3}	10^{-2}
2.5×10^{-5}	12.317	10.136	9.260	9.015	8.985	9.013
5×10^{-5}	12.373	10.155	9.263	9.013	8.987	9.014

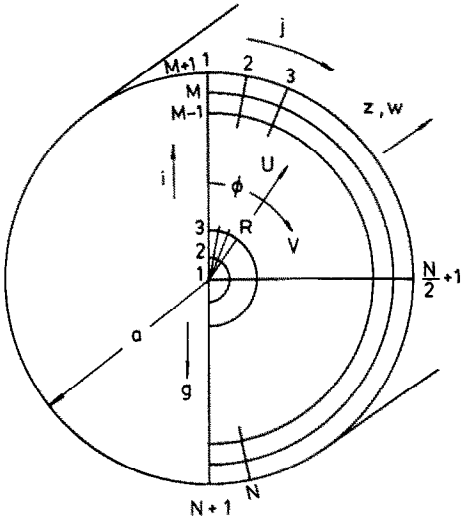

FIG. 1. Physical configuration and the coordinate system.

for which the secondary flow is weak. With the development of the secondary flow, the symmetry is lost and the location of $w = 0$ moves toward the lower wall as z increases from 2×10^{-3} to 6×10^{-3}. The location of $w = 0$ moves upward and the w profiles become more uniform as z further increases to $z = 5\times10^{-2}$ where the velocity profile is fully developed. Comparison of the results of $Pr = 2$ and 5, the effect of Prandtl number on the axial velocity due to buoyancy can be studied. One can observe that the curve of $Pr = 2$ at $z = 1\times10^{-3}$ almost coincides with that of $Pr = 5$, but the curve of $Pr = 2$ along $\phi = 0$ becomes more up-skewed at $z = 2\times10^{-3}$ and, furthermore, the maximum absolute values of w for $Pr = 2$ are higher than those for $Pr = 5$ at $z = 6\times10^{-3}$ and 1×10^{-2} due to the effect of stronger secondary flow with smaller Prandtl number.

The natural convection effect on the flow characteristic of the system is usually presented by the friction factor ratio $f\,Re/(f\,Re)_0$, where subscript 0 denotes the quantity for pure forced convection. Figure 4 shows the values of $f\,Re/(f\,Re)_0$ vs dimensionless axial distance z for the cases of $Pr = 0.7$, 2 and 5 with Rayleigh number as a parameter. When the Prandtl number is large, the axial velocity component w vanishes [4, 23–26]. Therefore, the line of $f\,Re/(f\,Re)_0 = 1.0$ is the result for the case of $Pr \to \infty$. The variation of the local friction factor ratio along the channel axis shows that the natural convection effect is negligible up to a certain axial distance z^*, depending mainly on the magnitude of the Grashof number and only slightly on the Prandtl number. When the value of Pr is fixed, the axial distance z^* is shorter with a high value of Ra, while the value of Ra is fixed, the axial distance z^* is shorter with a higher value of Pr. Each curve in Fig. 4 branches out from the line of $f\,Re/(f\,Re)_0 = 1$ at the onset point z^* and after reaching a maximum value, the curve approaches rapidly to a limiting value when the velocity profile becomes fully developed. Furthermore, one can observe that the curves with higher Pr fall below that of lower Pr for a fixed value of Ra. A special trend is also seen for the curve of $Pr(Ra) = 0.7(10^5)$. By a detailed inspection of the transverse velocity field u and v, multiple pair eddies appear at $z = 8\times10^{-3} \sim 1.4\times10^{-2}$ but finally single pair eddies are again obtained at $z \geqslant 2\times10^{-2}$. For the z range over which multiple pair eddies appear, $f\,Re/(f\,Re)_0$

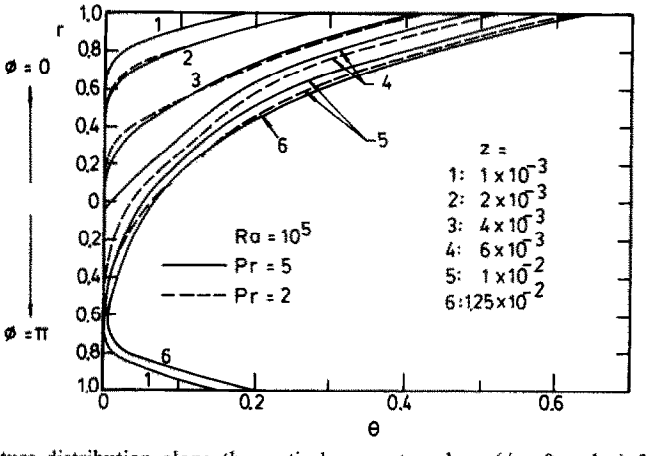

FIG. 2. Temperature distribution along the vertical symmetry plane ($\phi = 0$ and π) for $Pr = 5$ and 2 ($Ra = 10^5$).

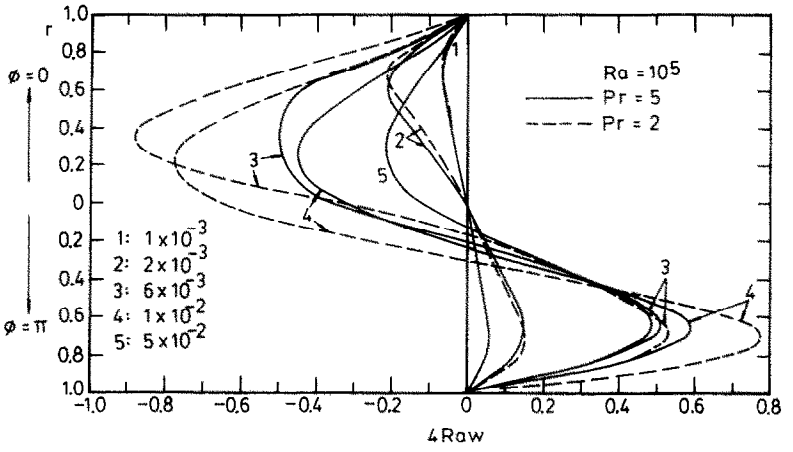

FIG. 3. Axial velocity profiles along the vertical symmetry plane ($\phi = 0$ and π) for $Pr = 5$ and 2 ($Ra = 10^5$).

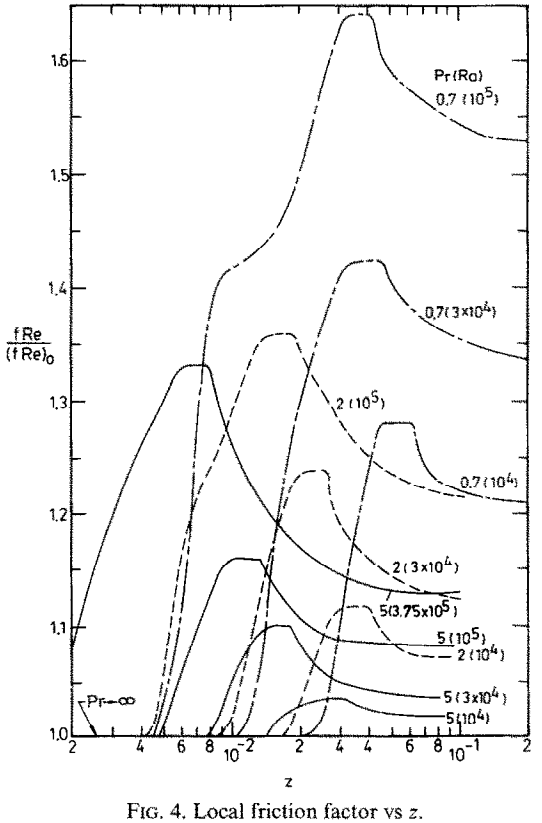

FIG. 4. Local friction factor vs z.

is retarded as seen in the corresponding curve in Fig. 4. Similar phenomena have been reported in refs. [37, 39]. However, an examination of this matter should consider stability analysis and is beyond the scope of the present work.

The local Nusselt number behavior is of primary interest. The effect of natural convection on the local Nusselt number for the thermal entrance flow is shown in Fig. 5 for the cases of $Pr = 0.7$, 2 and 5 with $Ra = 10^4$, 3×10^4, 10^5 and 3.75×10^5. The experimental data using water by Petukhov and Polyakov [19] and the numerical results based on the large Prandtl number assumption ($Pr \to \infty$) by Cheng and Ou [24] are also reproduced for comparison. It is seen that the curves with lower values of Pr fall below those with higher values of Pr for a given Rayleigh number. This phenomenon can be also seen in the previous experimental investigations using water and ethylene glycol in a glass tube by Morcos and Bergles [3] in the fully developed region, and the numerical results in ref. [36] in the thermal entrance region. One can also observe that the differences between the curves of $Pr \to \infty$ and $Pr = 0.7$ increase as the values of Ra increase. Although both Hong *et al.* [4] and Cheng and Ou [24] suggested that the analytical model based on the large Prandtl number assumption is approximately valid for water, the present results for $Pr = 5$ show a better agreement for the cases of $Ra = 2.1875 \times 10^4$ and 7.14×10^4. The experimental data fall above the curve of $Pr = 5$ and $Ra = 3.75 \times 10^5$. This phenomenon can be also seen in the comparison of experimental data and numerical results in ref. [38] in square channels. It may be caused by the effect of fluid property variation with temperature [1].

The variation of the local Nusselt number along the channel shows that the natural convection effect is negligible up to a certain axial distance z^* depending mainly on the magnitude of the Grashof number and also the Prandtl number. The values of z^* are seen to decrease with the increase in Ra. For a fixed Rayleigh number, the axial distance z^* decreases with the increase in Pr. The curve of the local Nusselt number is seen to deviate from that of the pure forced convection case. For the combined effect of entrance flow and natural convection, minimum and maximum local Nusselt numbers exist for some curves. Finally they approach asymptotic values when the temperature profiles become fully developed.

Because of the lack of additional data for the entrance flow, the asymptotic friction factor and Nusselt number results in the fully developed region are further compared with previous work. There were several different parameters chosen in the existing literature. After careful derivation, the relationships among the parameters are obtained as follows:

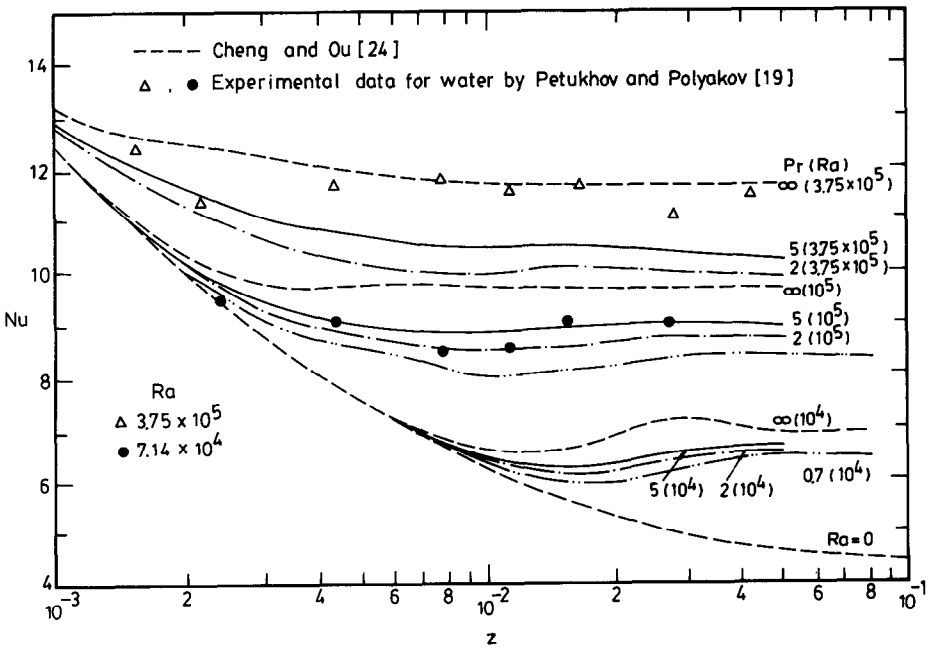

FIG. 5. Local Nusselt number vs z.

$$Re\,Ra_\tau = \left(\frac{2}{\pi}\right) Gr^+ \tag{19}$$

$$Ra^* = \frac{16Ra}{Nu} = \frac{4Pr\,Re\,Ra_\tau}{Nu} \tag{20}$$

where $Re\,Ra_\tau = \bar{W}(2a)/\nu \cdot g\beta(\partial T/\partial Z)a^4/\nu\alpha$ is the parameter used in refs. [8, 22], $Gr^+ = g\beta Q' a^3/k\nu^2$ is the parameter based on the rate of heat transfer per unit axial length and was used by Patankar *et al.* [37], and $Ra^* = g\beta(\bar{T}_w - T_b)d^3/\nu\alpha$ is the parameter based on the bulk temperature difference and was used by Morcos and Bergles [3]. In ref. [3] Ra_{fm} denoting the Rayleigh number Ra^* evaluated at the film temperature was also used. For the convenience of presenting experimental data [3], the parameters Ra^*_{fm} and Ra^* are used in Figs. 6 and 7, respectively.

It can be seen in Fig. 6 that the present asymptotic values of $f\,Re/(f\,Re)_0$ for $Pr = 5$ lie closely with the numerical result of $Pr = 4.5$ for uniform wall heat flux with zero heat conduction around the tube circumference [20]. The experimental data of water in glass and metal tubes [3] fall above the present result of $Pr = 5$ and lie between the IC and ZC curves [20] due to finite tube wall conduction around the circumference. The numerical results of $Pr = 4$ and 0.72 in ref. [22] fall above the present curves of $Pr = 5$ and 0.7, respectively, for the combination of the uniform axial heat flux and the uniform circumferential temperature thermal boundary condition. The numerical results of Patankar *et al.* [37] for the cases of $Pr = 5$ and 0.7 with bottom heating condition also fall above the present results accordingly. In view of the uniform axial and circumferential wall heat flux thermal boundary condition used in the present investigation, the present results of $Pr = 0.7$ are reasonable.

The asymptotic values of Nu in the present study are shown in Fig. 7. The results for $Pr = 5$ show a good agreement with the experimental data of water in a glass tube [3] and the ZC curve for $Pr = 4.5$ [20]. The IC prediction of $Pr = 0.72$ and 4 [22] lie above the present work of $Pr = 0.7$ and 5, respectively. The numerical results for $Pr = 5$ [37] with bottom heating condition predict higher values than the foregoing data. The correlation equation for air in a brass tube by Mori *et al.* [8] overestimates the data obtained by the present work for $Pr = 0.7$. By considering the trends of the data caused by the different boundary conditions, i.e. the use of a high conductivity wall material such as brass [8] and the zero wall conduction around the tube circumference used in this work, the present asymptotic Nusselt numbers for $Pr = 0.7$ are reasonable.

CONCLUDING REMARKS

(1) A relatively novel vorticity–velocity formulation of the Navier–Stokes equations and its numerical scheme are employed to study the natural convection effect on the Graetz problem in a horizontal tube without the aid of large Prandtl number assumptions. The values of the boundary vorticity on the tube wall are solved simultaneously with the velocity components u and v as shown in equation (17).

(2) The secondary flow distorts the axial velocity and temperature profiles, and the locations of the maximum velocity and the minimum fluid temperature are moved toward the bottom tube wall. For a given Rayleigh number, the effect of decreasing Prandtl number is to increase the distortion of the axial velocity and temperature profiles due to the stronger secondary flow.

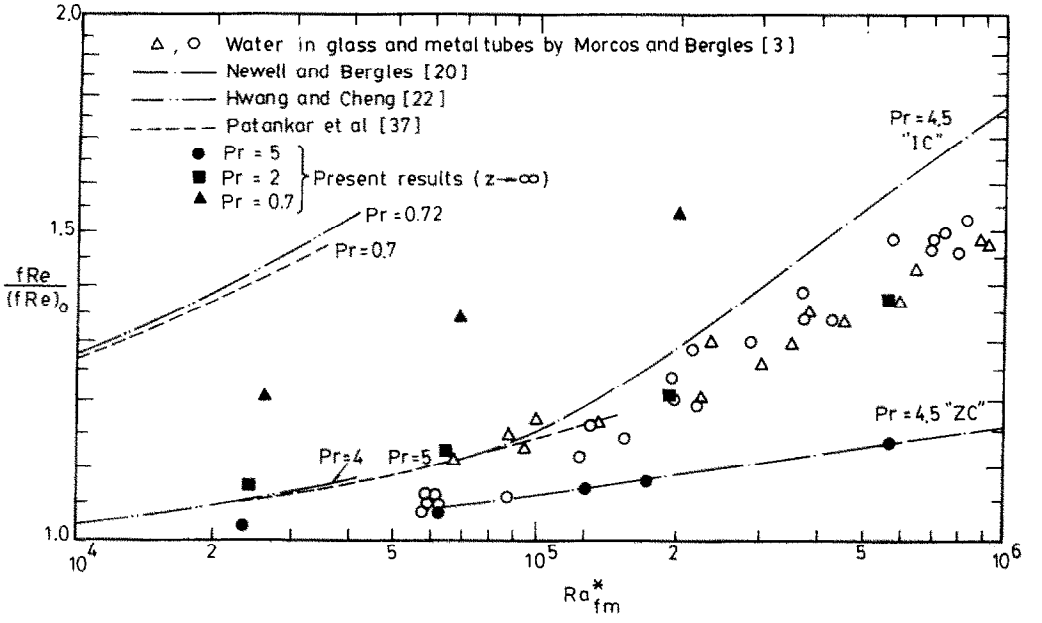

FIG. 6. Comparison of asymptotic friction factors with the existing theoretical and experimental data.

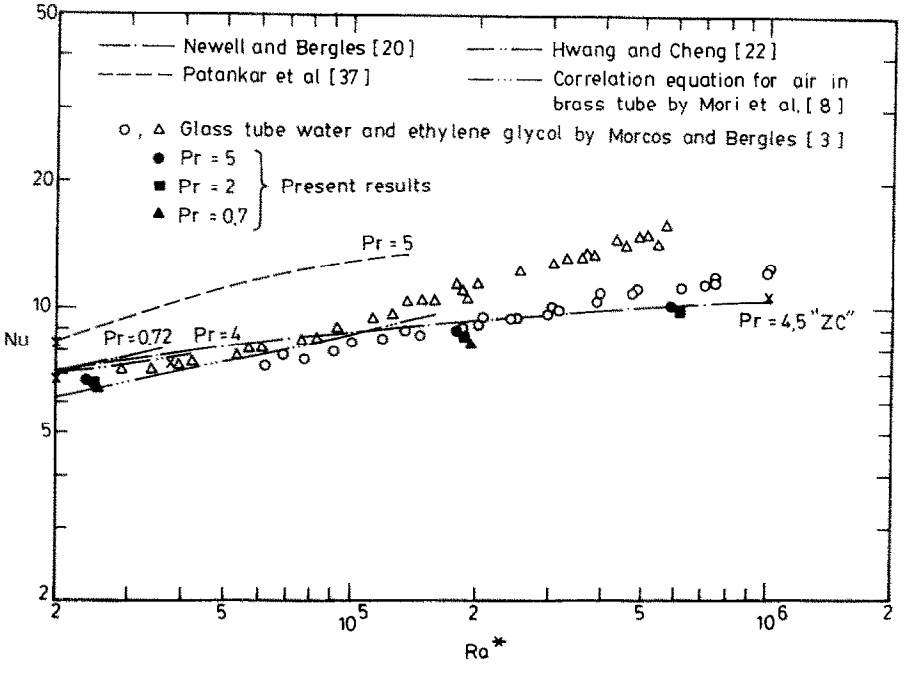

FIG. 7. Comparison of asymptotic Nusselt numbers with the existing theoretical and experimental data.

(3) Variations in both the local friction factor and Nusselt number show that the natural convection effect is negligible up to a certain axial distance, depending mainly on the magnitude of the Rayleigh number and to a lesser extent the Prandtl number. When the Prandtl number is held fixed, the axial distance is shortened with the increase in Rayleigh number. Likewise for a given Rayleigh number, the axial distance is also shortened with the increase in Prandtl number. Curves of the local friction factor ratio and local Nusselt number branch out from the curves for pure forced convection and, after reaching a maximum value for $f\,Re/(f\,Re)_0$ and a minimum or also a maximum value for Nu, the curves approach asymptotic values when the velocity and temperature profiles become fully developed. The curves of $f\,Re/(f\,Re)_0$ and Nu with higher values of Ra lie above that of the lower value of Ra. For a given Rayleigh number, the curve of Nu for the case of $Pr \to \infty$ attains the highest value, but the curve of $f\,Re/(f\,Re)_0$ with a lower value of Pr lies above that with the higher value of Pr due to the stronger secondary flow.

(4) The present results of $Pr = 5$ agree favorably with the available experimental and numerical data

both in the entrance and fully-developed flows. Because of a lack of corresponding data, the present ZC data of $Pr = 0.7$ are compared with the existing experimental and numerical results for the IC boundary condition to find a reasonable comparison.

Acknowledgement—The first author would like to thank the National Science Council of R.O.C. for its support of the present work through project NSC77-0401-E008-01.

REFERENCES

1. D. R. Oliver, The effect of natural convection on viscous-flow heat transfer in horizontal tubes, *Chem. Engng Sci.* **17,** 335–350 (1962).
2. C. A. Depew and S. E. August, Heat transfer due to combined free and forced convection in a horizontal and isothermal tube, *J. Heat Transfer* **93,** 380–384 (1971).
3. S. M. Morcos and A. E. Bergles, Experimental investigation of combined forced and free laminar convection in horizontal tubes, *J. Heat Transfer* **97,** 212–221 (1975).
4. S. W. Hong, S. M. Morcos and A. E. Bergles, Analytical and experimental results for combined forced and free laminar convection in horizontal tubes, *Proc. Fifth International Heat Transfer Conference*, Vol. 3, pp. 154–158, Tokyo (1974).
5. R. L. Shanon and C. A. Depew, Forced laminar flow convection in a horizontal tube with variable viscosity and free convection effects, *J. Heat Transfer* **91,** 251–258 (1969).
6. K. Kato, E. Watanabe, T. Ogura and T. Hanzawa, Effect of natural convection on laminar flow heat transfer in horizontal circular tubes, *J Chem. Engng Japan* **15**(5), 355–361 (1982).
7. J. A. Sabbagh, A. Aziz, A. S. El-Ariny and G. Hamad, Combined free and forced convection in inclined circular tubes, *J. Heat Transfer* **98,** 322–324 (1976).
8. Y. Mori, K. Futagami, S. Tokuda and M. Nakamura, Forced convective heat transfer in uniformly heated horizontal tube, 1st report—experimental study on the effect of buoyancy, *Int. J. Heat Mass Transfer* **9,** 453–463 (1966).
9. S. T. McComas and E. R. G. Eckert, Combined free and forced convection in a horizontal circular tube, *J. Heat Transfer* **88,** 147–153 (1966).
10. A. J. Ede, The heat transfer coefficient for flow in a pipe, *Int. J. Heat Mass Transfer* **4,** 105–110 (1961).
11. S. M. Morcos, M. M. Hilal, M. M. Kamel and M. S. Soliman, Experimental investigation of mixed laminar convection in the entrance region of inclined rectangular channels, *J. Heat Transfer* **108,** 574–579 (1986).
12. G. J. Hwang and J. P. Sheu, Liquid solidification in combined hydrodynamic and thermal entrance region of a circular tube, *Can. J. Chem. Engng* **54,** 66–71 (1976).
13. A. E. Bergles and R. R. Simond, Combined forced and free convection for laminar flow in horizontal tubes with uniform heat flux, *Int. J. Heat Mass Transfer* **14,** 1989–2000 (1971).
14. B. S. Petukhov, A. F. Polyakov and B. K. Strigin, Heat transfer in tubes with viscous-gravity flow, *Heat Transfer—Sov. Res.* **1,** 24–31 (1969).
15. C. A. Depew and R. C. Zenter, Laminar flow heat transfer and pressure drop with freezing at the wall, *Int. J. Heat Mass Transfer* **12,** 1710–1714 (1969).
16. R. D. Zerkle and J. E. Sunderland, The effect of liquid solidification in a tube upon laminar flow heat transfer and pressure drop, *J. Heat Transfer* **90,** 183–190 (1968).
17. R. L. Shannon and C. A. Depew, Combined free and forced laminar convection in a horizontal tube with uniform heat flux, *J. Heat Transfer* **90,** 353–357 (1968).
18. B. S. Petukhov and A. F. Polyakov, Effect of free convection on heat transfer during forced flow in a horizontal pipe, *High Temperature* **5,** 384–387 (1967).
19. B. S. Petukhov and A. F. Polyakov, Experimental investigation of gravitational fluid flow in a horizontal tube, *High Temperature* **5,** 75–81 (1967).
20. P. H. Newell and A. E. Bergles, Analysis of combined free and forced convection for fully developed laminar flow in horizontal tubes, *J. Heat Transfer* **92,** 83–89 (1970).
21. K. C. Cheng and S. W. Hong, Combined free and forced laminar convection in inclined tubes, *Appl. Scient. Res.* **27,** 19–38 (1972).
22. G. J. Hwang and K. C. Cheng, Boundary vorticity method for convective heat transfer with secondary flow—application to the combined free and forced laminar convection in horizontal tubes. In *Heat Transfer 1970/4*, Paper No. NC3.5. Elsevier, Amsterdam (1970).
23. K. C. Cheng, S. W. Hong and G. J. Hwang, Buoyancy effects on laminar heat transfer in the thermal entrance region of horizontal rectangular channels with uniform wall heat flux for large Prandtl number fluid, *Int. J. Heat Mass Transfer* **15,** 1819–1836 (1972).
24. K. C. Cheng and J. W. Ou, Free convection effects on Graetz problem for large Prandtl number fluids in horizontal tubes with uniform wall heat flux, *Proc. Fifth International Heat Transfer Conference*, Vol. 3, pp. 159–163 (1974).
25. J. W. Ou, K. C. Cheng and R. C. Lin, Natural convection effects on Graetz problem in horizontal rectangular channels with uniform wall temperature for large *Pr*, *Int. J. Heat Mass Transfer* **17,** 835–843 (1974).
26. J. W. Ou and K. C. Cheng, Natural convection effects on Graetz problem in horizontal isothermal tubes, *Int. J. Heat Mass Transfer* **20,** 953–960 (1977).
27. C. A. Hieber and S. K. Sreenivasan, Natural convection effects on Graetz problem in horizontal isothermal tubes, *Int. J. Heat Mass Transfer* **17,** 1337–1348 (1974).
28. L. S. Yao, Free–forced convection in the entry region of a heated straight pipe, *J. Heat Transfer* **100,** 212–219 (1978).
29. M. Hishida, Y. Nagano and M. S. Montesclaros, Combined forced and free convection in the entrance region of an isothermally heated horizontal pipe, *J. Heat Transfer* **104,** 152–159 (1982).
30. S. V. Patankar and D. B. Spalding, A calculation procedure for heat and mass transfer in three dimensional parabolic flows, *Int. J. Heat Mass Transfer* **15,** 1787–1806 (1972).
31. M. M. M. Abou-Ellail and S. M. Morcos, Buoyancy effects in the entrance region of horizontal rectangular channels, *J. Heat Transfer* **104,** 924–928 (1983).
32. B. Farouk and T. Fusegi, An evaluation of the vorticity–velocity formulation of the Navier–Stokes equations in predicting heat transfer problems, ASME paper 85-HT-8 (1985).
33. H. Fasel, Investigation of the stability of boundary layers by a finite-difference model of the Navier–Stokes equations, *J. Fluid Mech.* **78,** 355–383 (1976).
34. H. Fasel and O. Booz, Numerical investigation of supercritical Taylor-vortex flow for a wide gap, *J. Fluid Mech.* **138,** 21–52 (1984).
35. K. Ramakrishna, S. G. Rubin and P. K. Khosla, Laminar natural convection along vertical square ducts, *Numer. Heat Transfer* **5,** 59–79 (1982).
36. F. C. Chou and G. J. Hwang, Vorticity–velocity method for the Graetz problem and the effect of natural convection in a horizontal rectangular channel with uniform wall heat flux, *J. Heat Transfer* **109,** 704–710 (1987).
37. S. V. Patankar, S. Ramadhyani and E. M. Sparrow, Effect of circumferentially nonuniform heating on laminar combined convection in a horizontal tube, *J. Heat Transfer* **100,** 63–70 (1978).

38. F. C. Chou and G. J. Hwang, Experiments on combined free and forced laminar convection in horizontal square channels, *Proc. 2nd ASME JSME Thermal Engineering Joint Conference*, Vol. 4, pp. 135–141 (1987).

39. G. J. Hwang and M. J. Lin, Natural convection effects on laminar heat transfer in the thermal entrance region of horizontal isothermal tubes, *J. Chin. Inst. Engrs* **8**, 343–355 (1985).

ANALYSE NUMERIQUE DU PROBLEME DE GRAETZ AVEC CONVECTION NATURELLE DANS UN TUBE CHAUD HORIZONTAL

Résumé—Supposant un grand nombre de Prandtl, le problème de Graetz, avec effet de convection naturelle dans un tube horizontal uniformément chauffé, est étudié numériquement à l'aide d'une nouvelle méthode vorticité–vitesse. Des variations du coefficient de frottement local et du nombre de Nusselt en fonction du nombre de Rayleigh sont montrées pour des nombres de Prandtl $Pr = 5$, 2 et 0,7. Comparés à des données expérimentales pour l'eau, les résultats présentés pour $Pr = 5$ montrent un accord meilleur qu'avec $Pr \to \infty$. Les solutions asymptotiques pour $z \to \infty$ sont comparées avec les données analytiques et expérimentales disponibles. On observe un accord raisonnable.

NUMERISCHE UNTERSUCHUNG DES GRAETZ-PROBLEMS MIT ÜBERLAGERTER NATÜRLICHER KONVEKTION IN EINEM GLEICHFÖRMIG BEHEIZTEN WAAGERECHTEN ROHR

Zusammenfassung—Ohne Zuhilfenahme einer Beschränkung auf große Prandtl-Zahlen wird das Graetz-Problem mit überlagerter natürlicher Konektion in einem gleichförmig beheizten waagerechten Rohr numerisch mit einem relativ neuartigen Wirbelfunktions-Geschwindigkeits-Verfahren untersucht. Der Einfluß der Rayleigh-Zahl auf die örtlichen Werte von Wandschubspannung und Nusselt-Zahl wird für die Prandtl-Zahlen $Pr = 5$, 2 und 0,7 gezeigt. Vergleicht man die hier vorgestellten Ergebnisse für $Pr = 5$ mit den verfügbaren Versuchsdaten für Wasser, so zeigt sich eine bessere Übereinstimmung als für Berechnungen mit $Pr \to \infty$. Weiterhin werden die asymptotischen Lösungen für $z \to \infty$ mit vorhandenen analytischen und experimentellen Werten verglichen. Dabei ergibt sich eine verhältnismäßig gute Übereinstimmung.

ЧИСЛЕННЫЙ АНАЛИЗ ЗАДАЧИ ГРЭТЦА С УЧЕТОМ ЕСТЕСТВЕННОЙ КОНВЕКЦИИ В ОДНОРОДНО НАГРЕТОЙ ГОРИЗОНТАЛЬНОЙ ТРУБЕ

Аннотация—Задача Грэтца с учетом влияния естественной конвекции в однородно нагретой горизонтальной трубе решается численно в переменных скорость–завихренность методом, не использующим приближения больших чисел Прандтля. Зависимость локального коэффициента трения и числа Нуссельта от числа Рэлея приведена для чисел Прандтля $Pr = 5$, 2 и 0.7. Сравнение результатов, полученных для $Pr = 5$ с имеющимися опытными данными для воды показывает лучшее соответствие, чем для случая $Pr \to \infty$. Асимптотические решения для $z \to \infty$ сравниваются далее с существующими аналитическими и опытными данными. Найдено их хорошее соответствие.